Journal of Zhejiang University-SCIENCE C (Computers & Electronics)
ISSN 1869-1951 (Print); ISSN 1869-196X (Online)
www.zju.edu.cn/jzus; www.springerlink.com
E-mail: jzus@zju.edu.cn

Robust design of static synchronous series compensator-based stabilizer for damping inter-area oscillations using quadratic mathematical programming

Mahmoud Reza SHAKARAMI†, Ahad KAZEMI

(*Center of Excellence for Power System Automation and Operation, Department of Electrical Engineering, Iran University of Science and Technology, Tehran 16844, Iran*)

†E-mail: shakarami@iust.ac.ir

Received July 13, 2009; Revision accepted Nov. 26, 2009; Crosschecked Dec. 31, 2009

Abstract: This paper presents a procedure for designing a supplementary damping stabilizer for a static synchronous series compensator (SSSC) in multi-machine power systems. The objective is to shift the lightly damped inter-area modes toward the prescribed stability region. A lead-lag stabilizer is used to demonstrate this technique, in which a particular measure of stabilizer gain is considered as an objective function. Constraints of the problem for phase-lead and lag structures are derived. The objective function with the constraints is formed as a quadratic mathematical programming problem. For robust design, the parameters of the stabilizer are calculated under various operating conditions. Two types of SSSC-based stabilizer have been presented and designed. Numerical results including eigenvalue analysis and the nonlinear simulations on the 4- and 50-machine power systems are presented to show the effectiveness of the proposed method.

Key words: Inter-area oscillations, Static synchronous series compensator (SSSC), Damping stabilizer, Robust design, Quadratic mathematical programming

doi:10.1631/jzus.C0910428 **Document code:** A **CLC number:** TM761; TM721

1 Introduction

Inter-area oscillations, ranging from 0.1 to 0.7 Hz, are common phenomena in interconnected power systems. These oscillations appear from two or more groups of generators in different areas, swinging against each other. Inter-area oscillations are undesirable because they constrain the capability of power transmission, threaten system security, and damage the efficient operation of the power system. Therefore, it is desirable that these oscillations be damped efficiently. Conventionally, power system stabilizers (PSSs) are used for the damping of power system oscillations. However, the use of PSSs only may not be effective in providing sufficient damping for inter-area oscillations in some cases, particularly in cases with increasing transmission line loading over a long distance (Noroozian *et al*., 2001). Nowadays, series power electronics-based flexible AC transmission system (FACTS) controllers have become one of the best alternative means of improving damping power oscillations. The static synchronous series compensator (SSSC) is one of series FACTS devices that, in addition to increasing transferred power, can improve transient and small-disturbance stability of power systems (Gyugyi *et al*., 1997; Chen *et al*., 2003; Castro *et al*., 2004; 2007; Farsangi *et al*., 2004; Haque, 2005; Jowder, 2005; Kazemi *et al*., 2005). The SSSC is more effective for damping mechanical oscillations in comparison with the other FACTS devices (Castro *et al*., 2004). The SSSC injects a set of balanced voltages to transmission line quadrature with the line current. There are two control channels to control the magnitude and phase of the voltage, the magnitude

control channel and the phase control channel. When the SSSC is used for damping of mechanical oscillations, the damping stabilizer can be applied to both channels.

One of the effective methods of designing damping stabilizers in FACTS devices is linear programming (Pourbeik and Gibbard, 1996; 1998). In these works, researchers have calculated the phase of the stabilizer, and then assuming that the stabilizer phase remains constant in the frequency range of oscillation modes, they have calculated the gain of the stabilizer using a linear programming method. This assumption may not be true. In (da Cruz and Zanetta, 1997; Zanetta and da Cruz, 2005), gain and phase of PSS have been calculated simultaneously using mathematical programmings. The proposed method in these papers has been presented for a phase-lead stabilizer. However, to improve damping mechanical oscillations the stabilizer, in some cases particularly in the FACTS devices, may need a lag structure. Meanwhile, parameters of PSS in these papers have been calculated for certain operational conditions. However, a set of stabilizer parameters which stabilizes the system under a certain operational condition may not be satisfactory when there is a drastic change in the operational condition.

In this paper, a robust design of an SSSC-based stabilizer is presented as a quadratic mathematical programming problem. Constraints of the problem have been calculated for a phase-lead and a phase-lag stabilizer. The possible operational conditions that have significant effects on damping inter-area oscillations are simultaneously considered. Magnitude- and phase-based stabilizers as two types of the stabilizer are presented for SSSC. The stabilizers are designed for damping inter-area oscillations. The proposed method is used to design an SSSC-based stabilizer in a small and a large multi-machine power system.

2 Power system model

2.1 Generator

Depending on studying phenomena, goals, conditions and interesting time-scale, different approximations can be used to simplify modeling of synchronous machines. The nature of low frequency inter-area oscillations is related to the rotor of generators. Because of inertia, the rotation of rotors is relatively slow. Therefore, fast dynamics of stator and network is negligible in the study of inter-area oscillations. Usually sub-transient time constants are small in comparison with transient time constants. Therefore, the dynamics of dampers can be neglected yet still provide a good approximation. The turbine tends to be slow and the time constants of turbine/governor states can be relatively large. Therefore, it is supposed that mechanical power on shaft of turbines during a fault with a short clearing time is constant. This assumption is useful and it is used for most studies of angle stability in the power systems. According to the above assumptions, a fourth-order d-q axis model is used for a synchronous machine in this paper. This model can truly show the generators for studying inter-area oscillations. Nonlinear dynamic equations for each generator are presented in Appendix A.

2.2 Exciter

The IEEE type-AC-4A excitation system is considered in this work. Its block diagram is shown in Fig. 1. The roles of the used parameters for the system have been discussed in Anderson and Fouad (1977).

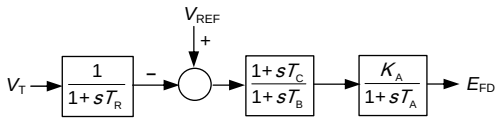

Fig. 1 Block diagram of the IEEE type-AC-4A excitation system

2.3 SSSC modeling

It is assumed that, in a multi-machine power system, an SSSC is installed on the transmission line between nodes 1 and 2 (Fig. 2).

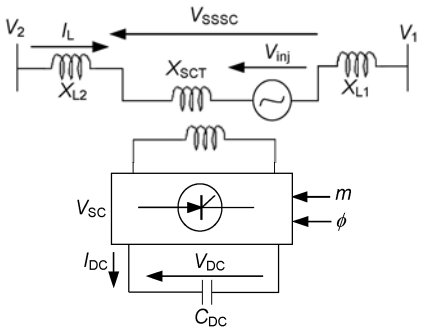

Fig. 2 Structure of the static synchronous series compensator (SSSC)

The SSSC consists of a series coupling transformer (SCT) with the leakage reactance X_{SCT}, a three-phase gate turn-off (GTO) based voltage source converter (VSC) and a DC capacitor. The SSSC can be described as (Wang, 1999)

$$V_{inj} = mkV_{DC}(\cos\phi + j\sin\phi), \quad (1)$$

$$I_L = I_D + jI_Q = |I_L|\angle\psi, \quad (2)$$

$$\frac{dV_{DC}}{dt} = \frac{mk}{C_{DC}}(I_D\cos\phi + I_Q\sin\phi), \quad (3)$$

where V_{inj} is the AC injected voltage by the SSSC; m and ϕ are the modulation ratio and phase defined by pulse width modulation (PWM), respectively; k is the ratio between the AC and DC voltage depending on the converter structure; V_{DC} is the DC voltage; C_{DC} is the DC capacitor value; I_D and I_Q are D and Q components of the line current I_L, respectively.

3. SSSC-based stabilizers

3.1 Phase-based stabilizer

Assuming a lossless SSSC, the AC voltage is kept in quadrature with the line current, so that the SSSC exchanges only reactive power with the transmission line. By adjusting the magnitude of the injected voltage, the reactive power exchange can be controlled. When the SSSC voltage lags the line current by 90º, it emulates a series capacitor. It can also emulate a series inductor when the voltage leads the line current by 90º. Thus, an SSSC can be considered as a series reactive compensator where the degree of compensation can be varied by controlling the magnitude of the injected voltage. In this study, the SSSC is considered in capacitor mode. To keep the injected voltage in quadrature with the line current, a proportional-integral (PI) controller (Fig. 3) has been used. Here ϕ_{ref} is the phase of the injected voltage in steady state and is defined as $\phi_{ref}=-90^o+\psi_{ss}$, where ψ_{ss} is the angle of the line current in steady state, T_{SSSC} is the time constant of the converter, and K_P and K_I are the proportional and integral gain of the PI controller, respectively. A lead-lag stabilizer for damping inter-area oscillations is included in the PI controller. In this case, the stabilizer is called the phase-based stabilizer and for convenience written as the 'ϕ-based stabilizer'. In this stabilizer, T_w is a time constant usually in the range of 1–15 s. To design a stabilizer, the value of T is usually assumed pre-specific, and x_2, x_1, and x_0 are parameters to be determined. In this study, the value of T adopted for the stabilizer is considered according to the typical values in previous studies particularly in (Anderson and Fouad, 1977; Sauer and Pai, 1998).

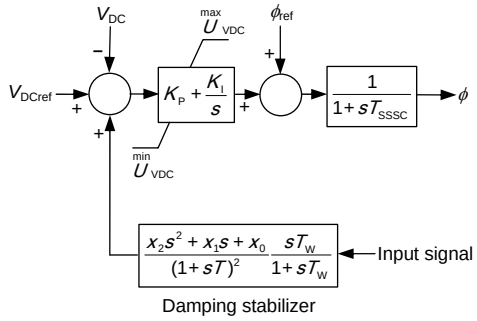

Fig. 3 Block diagram of the static synchronous series compensator (SSSC) phase controller with a damping stabilizer

The feedback signal for the stabilizer is selected amongst local signals as the line current, the line real power, and the line reactive power.

3.2 Magnitude-based stabilizer

To control the magnitude of the injected voltage, modulation ratio m can be controlled. Fig. 4 shows the block diagram of the controller in this case. Here, m_{ref} is the modulation ratio in the steady state condition and its value is considered as $m_{ref}=X_{ref}I_{ss}$, where I_{ss} is the line current in steady state and X_{ref} is the reactance produced by the SSSC in steady state. A stabilizer for damping of inter-area oscillations is included in the magnitude controller. This stabilizer is the m-based stabilizer.

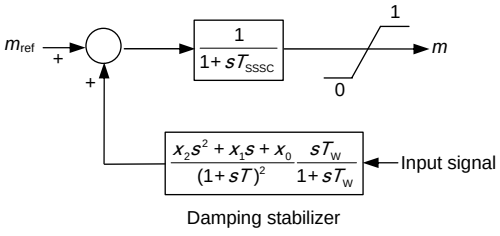

Fig. 4 Block diagram of the static synchronous series compensator (SSSC) magnitude controller with a damping stabilizer

4 Stabilizer design

The method adopted in this work is an extension to the method proposed by Zanetta and da Cruz (2005), taking into account a phase-lag stabilizer for SSSC. This method is summarized as follows: In the first step, the closed-loop system is considered as in Fig. 5a, where $\boldsymbol{G}$ and $\bar{\boldsymbol{F}}$ are the power system transfer matrix and the stabilizer transfer matrix, respectively. In the second step, the stabilizer transfer matrix is changed by $\Delta\boldsymbol{F}$. In this case, the closed-loop system change is shown in Fig. 5b, where $\bar{\boldsymbol{G}}$ is the transfer matrix of the inner loop between $\boldsymbol{G}$ and $\bar{\boldsymbol{F}}$. In Fig. 5, U_{ref} is the input signal of the system. U_{ref} is replaced by V_{DCref} and m_{ref} for the phase- and magnitude-based stabilizers, respectively. One of the local signals is selected as the feedback signal for the stabilizer. $\Delta\boldsymbol{F}$ is calculated to shift eigenvalues of critical modes to the desired values.

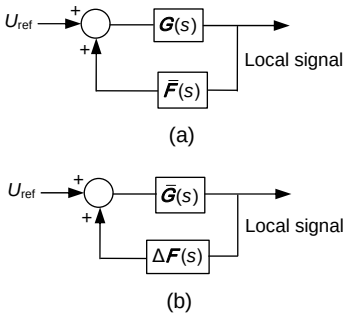

Fig. 5 Closed-loop system (a) in the first step and (b) in the second step

In the following, a procedure for calculating $\Delta\boldsymbol{F}$ is presented. Assuming that variations of $\Delta\boldsymbol{F}$ is sufficiently small, the variation of the eigenvalues can be approximated as

$$\Delta\lambda_i^p = \rho_i^p \Delta f(\lambda_i^p), \quad i = 1,\ 2,\ ...,\ n, \tag{4}$$

where n is the number of the critical eigenvalues; p is the point of operation; ρ_i^p is the residue associated to the ith eigenvalue of $\bar{G}$ under the pth operation condition. Eq. (4) can be rewritten as

$$\begin{aligned}\Delta\lambda_i^p = &\left(\mathrm{Re}(\rho_i^p)\,\mathrm{Re}\left(\Delta f(\lambda_i^p)\right) - \mathrm{Im}(\rho_i^p)\,\mathrm{Im}\left(\Delta f(\lambda_i^p)\right)\right)\\ &+ \mathrm{j}\left(\mathrm{Re}(\rho_i^p)\,\mathrm{Im}\left(\Delta f(\lambda_i^p)\right) + \mathrm{Im}(\rho_i^p)\,\mathrm{Re}\left(\Delta f(\lambda_i^p)\right)\right).\end{aligned} \tag{5}$$

It is assumed that the stabilizer has a lead-lag structure as follows:

$$f(s) = \frac{x_2 s^2 + x_1 s + x_0}{(1+sT)^2}\frac{sT_{\text{w}}}{1+sT_{\text{w}}}. \tag{6}$$

By substituting $s = \lambda_i^p$ and $x_z = \Delta x_z$ (z=1, 2, 3) in Eq. (6), the real and imaginary part variations of $\Delta f(\lambda_i^p)$ are

$$\mathrm{Re}\left(\Delta f(\lambda_i^p)\right) = R_{2i}^p \Delta x_2 + R_{1i}^p \Delta x_1 + R_{0i}^p \Delta x_0, \tag{7}$$

$$\mathrm{Im}\left(\Delta f(\lambda_i^p)\right) = I_{2i}^p \Delta x_2 + I_{1i}^p \Delta x_1 + I_{0i}^p \Delta x_0, \tag{8}$$

where R_{2i}^p, R_{1i}^p, R_{0i}^p, I_{2i}^p, I_{1i}^p, and I_{0i}^p are specified values. To shift critical eigenvalues to the left of the imaginary axis, we must have

$$\mathrm{Re}(\Delta\lambda_i^p) \le -\left|\Delta\sigma_i^p\right|, \tag{9}$$

$$-\left|\Delta\omega_i^p\right| \le \mathrm{Im}(\Delta\lambda_i^p) \le \left|\Delta\omega_i^p\right|, \tag{10}$$

where $\Delta\sigma_i^p$ and $\Delta\omega_i^p$ are the desired shift values of the real part and acceptable frequency variations of the critical eigenvalue λ_i^p, respectively. By substituting Eqs. (7) and (8) in Eq. (5), we can obtain $\Delta\lambda_i^p$ as a linear function from Δx_2, Δx_1, and Δx_0. Then, substituting the real part of $\Delta\lambda_i^p$ in Eq. (9) and its imaginary part in Eq. (10) yields

$$\alpha_{2i}^p \Delta x_2 + \alpha_{1i}^p \Delta x_1 + \alpha_{0i}^p \Delta x_0 \le -\left|\Delta\sigma_i^p\right|, \tag{11}$$

$$-\left|\Delta\omega_i^p\right| \le \beta_{2i}^p \Delta x_2 + \beta_{1i}^p \Delta x_1 + \beta_{0i}^p \Delta x_0 \le \left|\Delta\omega_i^p\right|, \tag{12}$$

where α_{2i}^p, α_{1i}^p, α_{0i}^p, β_{2i}^p, β_{1i}^p, and β_{0i}^p are specified values. On the other hand, if the angle of residue ρ_i^p is positive, the stabilizer must have a phase-lead characteristic. Otherwise, it must have a phase-lag characteristic. Considering $\hat{x}_2 = \dfrac{x_2}{x_0 T^2}$, $\hat{x}_1 = \dfrac{x_1}{x_0 T}$, and $\bar{s} = sT$ and substituting them in Eq. (6) yields

$$f(\bar{s}) = x_0 \frac{\hat{x}_2 \bar{s}^2 + \hat{x}_1 \bar{s} + 1}{(1+\bar{s})^2}\frac{T_{\text{w}}\bar{s}}{T + T_{\text{w}}\bar{s}}. \tag{13}$$

According to Dorf and Bishop (2005) for a phase-lead structure, it is assumed that zeroes of $f(\bar{s})$ are almost one-decade nearer to the center than that of its poles (i.e., they belong to interval[−1, −0.1]) and for the phase-lag structure, the zeroes are almost one decade further to the center (i.e., they belong to interval[−10, −1]). This is graphically shown for lead and lag structures in Fig. 6, in which the points inside the triangles and above the parabolas correspond to the above intervals. To represent the constraints as a linear function, the parabolas are approximated by lines. In this case, the zeros may be complex values, but the real parts of the complex zeros are located in the above intervals.

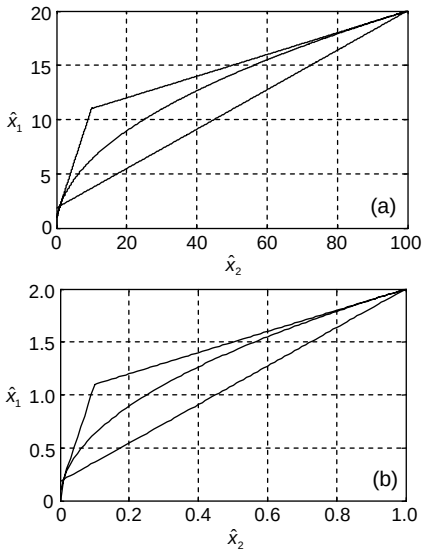

Fig. 6 Region corresponding to (a) phase-lead and (b) phase-lag stabilizers

According to Fig. 6a, the constraints for phase-lead structure can be written as (Zanetta and da Cruz, 2005)

$$\hat{x}_1 - \hat{x}_2 \le 1, \tag{14}$$

$$\hat{x}_1 - 0.1\hat{x}_2 \le 10, \tag{15}$$

$$-99x_1 + 18x_2 \le -180. \tag{16}$$

As shown in Fig. 6b, the constraints for the phase-lag stabilizer are

$$\hat{x}_1 - \hat{x}_2 \le 1, \tag{17}$$

$$10\hat{x}_1 - 100\hat{x}_2 \le 1, \tag{18}$$

$$-99\hat{x}_1 + 180\hat{x}_2 \le -18. \tag{19}$$

Substituting $\hat{x}_2$ and $\hat{x}_1$ in Eqs. (14)–(19) and assuming $x_z = \Delta x_z + \bar{x}_z$ (z=1, 2, 3, …), where $\bar{x}_0$, $\bar{x}_1$, and $\bar{x}_2$ are known values, the constraints can be rewritten for lead structure as Eqs. (20)–(22) and for lag structure as Eqs. (23)–(25):

$$-\Delta x_2 + T\Delta x_1 - T^2\Delta x_0 \le \bar{x}_2 - T\bar{x}_1 + T^2\bar{x}_0, \tag{20}$$

$$-\Delta x_2 + 10T\Delta x_1 - 100T^2\Delta x_0 \le \bar{x}_2 - 10T\bar{x}_1 + 100T^2\bar{x}_0, \tag{21}$$

$$18\Delta x_2 - 99T\Delta x_1 - 180T^2\Delta x_0 \le -18\bar{x}_2 + 99T\bar{x}_1 + 180T^2\bar{x}_0, \tag{22}$$

$$-\Delta x_2 + T\Delta x_1 - T^2\Delta x_0 \le \bar{x}_2 - T\bar{x}_1 + T^2\bar{x}_0, \tag{23}$$

$$-100\Delta x_2 + 10T\Delta x_1 - T^2\Delta x_0 \le 100\bar{x}_2 - 10T\bar{x}_1 + T^2\bar{x}_0, \tag{24}$$

$$180\Delta x_2 - 99T\Delta x_1 + 18T^2\Delta x_0 \le -180\bar{x}_2 + 99T\bar{x}_1 - 18T^2\bar{x}_0. \tag{25}$$

The following function, as the gain of the stabilizer at the frequency $\bar{\omega}_q$ (q=1, 2, ..., N) is considered as the objective function (Zanetta and da Cruz, 2005). This index represents one possible measure of the stabilizer gain. Loop gain of the stabilizer and consequently its control cost is reduced by minimization of this index. As a criterion, to achieve a similar damping ratio for a critical oscillation mode, the stabilizer with lower loop gain is more valuable.

$$J = \min \sum_{q=1}^{N} \left| f(\mathrm{j}\bar{\omega}_q) \right|^2, \tag{26}$$

where $\bar{\omega}_1$, $\bar{\omega}_2$, ⋯, $\bar{\omega}_N$ are a set of frequencies in the complex plane where the critical eigenvalue must be shifted.

By substituting Eq. (6) in Eq. (26) and considering s=j$\bar{\omega}_i$ and $\boldsymbol{X} = \bar{\boldsymbol{X}} + \Delta\boldsymbol{X}$, we can easily rewrite the objective function as

$$J = \min\left(\frac{1}{2}\Delta\boldsymbol{X}^{\mathrm{T}}\boldsymbol{H}\Delta\boldsymbol{X} + \boldsymbol{f}^{\mathrm{T}}\Delta\boldsymbol{X} \right), \tag{27}$$

where the matrix $\boldsymbol{H}$, vector $\boldsymbol{f}$ and vector $\bar{\boldsymbol{X}} = [\bar{x}_2\ \bar{x}_1\ \bar{x}_0]^{\mathrm{T}}$ are known and $\Delta\boldsymbol{X} = [\Delta x_2\ \Delta x_1\ \Delta x_0]^{\mathrm{T}}$ is the unknown vector to be tuned. Eq. (27) with constraints Eq. (11) and Eq. (12) and Eqs. (20)–(22) or

Eqs. (23)–(25) is considered as a quadratic mathematical programming problem. To solve this problem the 'quadprog' algorithm provided by the Matlab Optimization Toolbox is applied here. The proposed approach is an iterative method. In this method, the calculated vector of $\Delta \boldsymbol{X}$ is added to the known vector $\overline{\boldsymbol{X}}$ and it is considered as the known vector in the next iteration. The vector $\overline{\boldsymbol{X}}$ in the first iteration is set to zero.

5 Simulation results

The cases studied here are 2-area 4-machine and 2-area 50-machine power systems as small and large power systems, respectively.

5.1 Robust design of the SSSC-based stabilizer in the 4-machine power system

A single line diagram of the system is shown in Fig. 7 (Liu, 2006). To control inter-area oscillations, an SSSC is installed in the tie-line between nodes 5 and 6. Specific parameters used for the SSSC, generators and network are given in Appendix B. The loads are modeled as constant impedances.

In this system, five operating scenarios based on the transmitted power between the interconnected areas and outages of lines are investigated. To increase the transferred power, with no variation of reactive power of loads, the real power of the load in area 2 has been increased and then the real power of the load in area 1 has been modified to achieve a given tie-line transferred power.

The summary of operating conditions studied in this work is shown in Table 1.

The parameters of PI controller are calculated as follows:

Table 1 Operating conditions considered in the 4-machine power system

Operating condition	Characteristics	Transmitted power, P (MW)
1	Light loading: L_1=11.1 MW, L_2=11.9 MW	190
2	Nominal loading: L_1=9.2 MW, L_2=13.8 MW	380
3	Heavy loading: L_1=8.9 MW, L_2=14.1 MW	410
4	Nominal loading with outage one line between nodes 2 and 5	375
5	Heavy loading with outage one line between nodes 3 and 4	410

To obtain a suitable response for the system at a certain operational condition, for a positive value of K_I, the value of K_P is increased so that the modes related to phase-controller (controller modes) are stable. Meanwhile, the PI controller has no significant degraded effects on damping mechanical oscillations. Then, the values that are suitable for all considered operation conditions are selected. For the operational conditions presented in Table 1, K_P and K_I are approximately calculated as $25 \le K_P \le 120$ and $200 \le K_I \le 450$.

Considering K_P=25 and K_I=200, the inter-area mode in the open-loop system for different operating conditions are shown in Table 2. It is clear that the damping ratio of inter-area mode is noticeably reduced and it is close to the instability point by increasing transmitted power.

An SSSC stabilizer to improve the damping of inter-area oscillations is designed in this section. For comparison, the parameters of the ϕ-based and the m-based stabilizers are calculated. According to the design method, a signal with the maximum residue for the inter-area mode is selected as the feedback signal for the damping stabilizer.

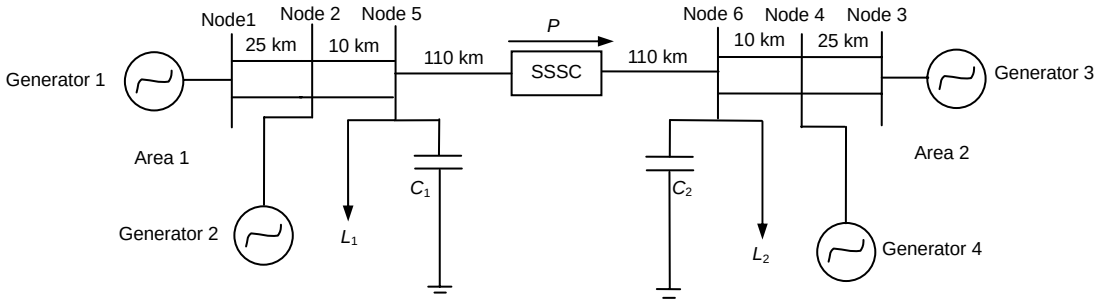

Fig. 7 One-line diagram of the 4-machine power system

Table 2 Inter-area mode in an open-loop system for the 4-machine power system

Operating condition	Eigenvalue	ζ (%)
1	−0.436±j2.924	14.748
2	−0.183±j1.640	11.089
3	−0.0469±j1.838	2.551
4	−0.081±j1.559	5.188
5	−0.015±j1.792	0.837

Table 3 shows residues for the inter-area mode for different operational conditions. It can be seen from Table 3 that:

1. When the stabilizer is applied for the phase control channel (the ϕ-based stabilizer), the residues for the inter-area mode for different local feedback signals are higher than when the stabilizer is used for the magnitude control channel (the *m*-based stabilizer).

2. Angles of residues for the *m*-based stabilizer are positive and for the ϕ-based stabilizer are negative, therefore the *m*-based stabilizer must have a lead structure and the ϕ-based stabilizer must have a lag structure.

3. Variation of the current in the transmission line, where the SSSC is installed, is the best signal for both stabilizers.

Considering the line current as the feedback signal, the magnitude of residue for inter-area mode for K_I=200 and different values of K_P is shown in Fig. 8a. Also, the magnitude of residues for inter-area mode for K_P=25 and different values of K_I is shown in Fig. 8b. It was confirmed that for different acceptable values of K_P and K_I, the magnitude of residues for inter-area mode for the SSSC ϕ-based stabilizer is higher than that of the *m*-based stabilizer.

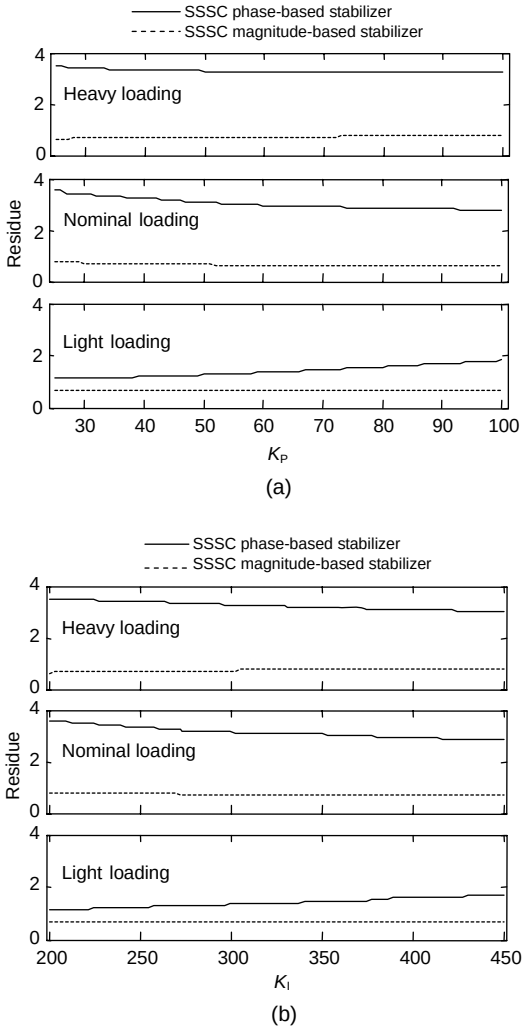

Fig. 8 Magnitude of residue for inter-area mode with (a) K_I=200 and (b) K_p=25 (line current as feedback signal)

Table 3 Residues for inter-area mode for different signals in the 4-machine power system

Operating condition	SSSC-based damping stabilizer	Input signal		
		ΔI	ΔP	ΔQ
1	ϕ-based	1.13∠−77.230°	0.99∠−78.480°	0.41∠−75.320°
	m-based	0.65∠84.920°	0.61∠84.440°	0.21∠83.610°
2	ϕ-based	3.57∠−110.20°	2.04∠−126.69°	3.18∠−105.49°
	m-based	0.75∠112.40°	0.43∠95.910°	0.67∠117.11°
3	ϕ-based	3.46∠−153.23°	1.16∠−176.38°	3.23∠−151.76°
	m-based	0.64∠105.03°	0.28∠87.430°	0.65∠106.16°
4	ϕ-based	3.36∠−132.03°	1.043∠−150.60°	3.30∠−131.28°
	m-based	0.55∠101.85°	0.24∠83.29°	0.54∠102.6°
5	ϕ-based	3.184∠−149.75°	1.15∠−171.57°	3.05∠−150.82°
	m-based	0.59∠102.39°	0.21∠80.57°	0.56∠101.33°

It was assumed that the desired minimum damping ratio for the inter-area mode in each operational condition was ζ=20%. According to the frequency of oscillation modes in the open-loop system, the value of $\overline{\omega}_q$ in Eq. (26) had been set to 1, 3, 4 rad/s. The time constant of the stabilizer was set as T=0.4 s. Also, the effects of the stabilizer on other modes must be considered, so that the damping ratios of other modes have been increased or do not become less than a specific value and the variations of their frequencies must be acceptable. To improve the damping ratio of inter-area mode to a desired value, the parameters of the proposed robust stabilizer were calculated and shown in Table 4. These values show that the loop gains of the ϕ-based stabilizer were smaller than those of the m-based stabilizer. In other words, the ϕ-based stabilizer was more effective for damping inter-area oscillations.

Table 4 Parameters of the proposed robust stabilizers in the 4-machine power system

SSSC-based stabilizer	x_2	x_1	x_0	$\lvert f(\mathrm{j}\omega)\rvert$
m-based	0.256 57	0.340 79	0.069 16	0.7165
ϕ-based	0.006 59	0.052 07	0.142 61	0.0952

The loop gains of stabilizers ($|f(\mathrm{j}\omega)|$) were typically calculated at a frequency of ω=2 rad/s

Inter-area mode in the closed-loop system for different operational conditions (Tables 5 and 6) show that the damping ratio of the inter-area mode has been improved to the desired value.

For completeness and verification of the designed stabilizers, a three-phase fault was applied to the test system at bus 6 with a fault duration of 0.02 s. The fault was cleared without line switching.

Since generators 1 and 3 have the most contribution in the inter-area mode, typically the swing angle of generator 1 with respect to generator 3, for operation conditions 3 and 5 are shown in Fig. 9. It shows that the SSSC-based stabilizers can effectively damp inter-area oscillations.

5.2 Robust design of the SSSC-based stabilizer in a 50-machine power system

The 50-machine power system was a moderately sized system that included all the modeling features and the complexity of a large-scale power system.

Table 5 Closed-loop inter-area mode in an SSSC ϕ-based stabilizer for the 4-machine power system

Operating condition	Eigenvalue	ζ (%)
1	−1.218±j3.111	36.45
2	−0.376±j1.362	26.61
3	−0.405±j1.685	23.37
4	−0.310±j1.412	21.44
5	−0.335±j1.634	20.08

Table 6 Closed-loop inter-area modes in an SSSC m-based stabilizer for the 50-machine power system

Operating condition	Eigenvalue	ζ (%)
1	−1.298±j3.024	39.44
2	−0.421±j1.438	28.09
3	−0.408±j1.689	23.48
4	−0.335±j1.594	20.56
5	−0.334±j1.625	20.13

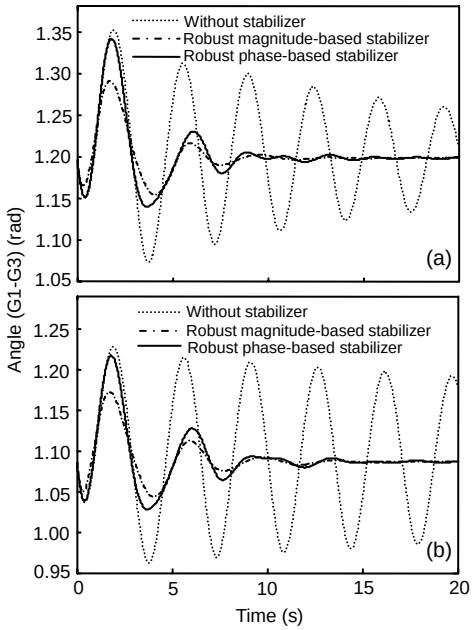

Fig. 9 Swing angle of generator 1 with respect to generator 3 for operation (a) condition 3 and (b) condition 5

This system contained 44 generators represented by a classical model and 6 generators represented by a two-axis model and equipped with an exciter. No PSS was installed in the system. The system data was given in (Vittal, 1992; Liu, 2006). Loads were modeled as constant impedances. The operational conditions were characterized by increasing the real power generation at buses 93 and 110 without any variation in loads of the system. Amongst transmission lines,

outage of lines 2–6 has the most effect on the reduction of damping critical inter-area mode. Operating conditions in Table 7 were considered for robust design of the system. For different operational conditions, the load flow was undertaken and eigenvalues of the system were calculated.

Table 7 Considered operating conditions in the 50-machine power system

Operating condition	Characteristics
1	Light loading: P_{g93}, P_{g110}=1100 MW
2	Nominal loading: P_{g93}, P_{g110}=1400 MW
3	Heavy loading: P_{g93}, P_{g110}=1700 MW
4	Nominal loading with outage lines 2–6

Table 8 shows inter-area modes of this system for each operational condition. By increasing the generation level at buses 93 and 110, it can be seen that the damping ratio of inter-area mode 1 with the frequency around 0.42 Hz decreased but the damping ratio of inter-area mode 2 with a frequency close to 0.65 Hz was approximately constant. Therefore, inter-area mode 1 was considered as a critical mode and the goal of the SSSC was to improve damping of the mode.

Table 8 Inter-area modes in an open-loop system for the 50-machine power system

Operating condition	Eigenvalue		ζ (%)	
	Mode 1	Mode 2	Mode 1	Mode 2
1	−0.036±j2.765	−0.202±j4.099	1.30	4.92
2	−0.015±j2.664	−0.198±j4.081	0.57	4.84
3	0.017±j2.524	−0.193±j4.055	−0.69	4.75
4	0.002±j2.595	−0.191±j4.055	−0.08	4.70

In this system, the variation of the line current magnitude was considered to be the feedback signal. The best installing location for the SSSC was selected in the residue analysis. By calculating residues in different locations in the studying system, the line 66-63 was selected as the optimal location for the SSSC.

The purpose of the SSSC-based stabilizer in this power system is to increase the damping ratio of inter-area mode 1 to a maximum possible value. In Eq. (26), we set $\overline{\omega}_q$=1, 3, 4 rad/s and T=0.4 s. Parameters of the robust stabilizer are shown in Table 9.

The closed-loop inter-area modes are shown in Table 10. It can be seen that the damping ratio of critical inter-area mode for different operational conditions had been improved. Also, the stabilizer had no significant effect on non-critical inter-area mode. Moreover, the ϕ-based stabilizer, compared with the m-based stabilizer, was more effective for damping critical inter-area oscillations.

Table 9 Parameters of robust SSSC damping stabilizers in the 50-machine power system

SSSC-based stabilizer	x_2	x_1	x_0
m-based	0.034 46	0.116 23	0.098 00
ϕ-based	0.076 05	0.349 60	0.423 80

Table 10 Closed-loop inter-area modes in SSSC-based stabilizers for the 50-machine power system

Operating condition	SSSC-based stabilizer	Eigenvalue		ζ (%)	
		Mode 1	Mode 2	Mode 1	Mode 2
1	ϕ-based	−0.195± j2.824	−0.217± j4.137	6.89	5.24
	m-based	−0.072± j2.785	−0.214± j4.107	2.58	5.20
2	ϕ-based	−0.213± j2.711	−0.212± j4.119	7.83	5.14
	m-based	−0.053± j2.684	−0.209± j4.088	1.97	5.11
3	ϕ-based	−0.279± j2.534	−0.195± j4.102	10.9	4.75
	m-based	−0.022± j2.545	−0.202± j4.062	0.86	4.97
4	ϕ-based	−0.172± j2.633	−0.194± j4.081	6.52	4.75
	m-based	−0.033± j2.615	−0.198± j4.061	1.26	4.87

To demonstrate the effectiveness of the proposed stabilizers in the 50-machine power system, a three-phase fault was applied on bus 7 for a duration of 0.03 s. The fault is cleared without the line tripping. Since generators 93, 95, and 145 had the most contribution in the oscillations of the critical mode, typically the swing angle of generator 93 with respect to generator 145 when the generation level at buses 93 and 110 was set to 1600 MW, is shown in Fig. 10. It can be seen that the SSSC damping stabilizer can effectively damp inter-area oscillations.

A comparative study between the method of (da Cruz and Zanetta, 1997; Zanetta and da Cruz, 2005) and ours to design PSS showed that, for power systems in the presence of FACTS devices to improve

damping mechanical oscillations, the stabilizer may need a lag structure instead of a leading structure. On the other hand, it was feasible that the parameters of the stabilizer can be robust with variations of operational conditions. Moreover, comparisons of our results with those of (Wang, 1999; Kazemi *et al*., 2005; Castro *et al*., 2007) revealed that the SSSC-phase based stabilizer can effectively damp mechanical oscillations, even more effectively than that of the magnitude-based stabilizer.

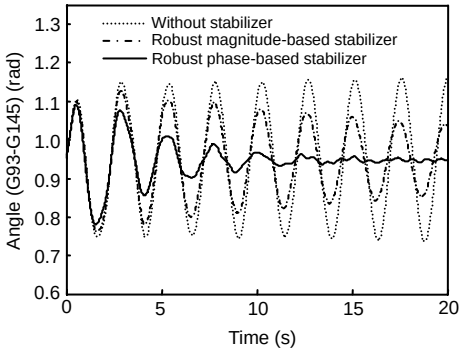

Fig. 10 Swing angle of generator 93 with respect to generator 145 for P_{g93}=P_{g110}=1600 MW

6 Conclusion

The use of quadratic mathematical programming to design a robust SSSC-based stabilizer for a power system working at various operational conditions is studied in this paper. In this method, the gain and the phase of the stabilizer are calculated simultaneously. The objective function is considered as a particular measure of the stabilizer gain. Constraints of the problem are derived for lead and lag structures. The best location and feedback signal for the SSSC-based stabilizer are selected in residue analysis. Magnitude- and phase-based stabilizers as two types of stabilizer are presented for the SSSC. The suggested robust design technique is successfully applied for an SSSC installed in a small and large multi-machine power system for damping inter-area oscillations. Performance of the robust stabilizer, tuned using the suggested technique, is verified through eigenvalue analysis and nonlinear simulation results. Results show that when the SSSC stabilizer is used for phase control channel, in comparison with the magnitude control channel, it is more effective for damping inter-area oscillations.

References

Anderson, P.M., Fouad, A.A., 1977. Power System Control and Stability. Iowa State University Press, Iowa, USA, p.233-308.

Castro, M.S., Nassif, A.B., da Costa, V.F., da Silva, L.C.P., 2004. Impacts of FACTS Controllers on Damping Power Systems Low Frequency Electromechanical Oscillations. Transmission and Distribution Conf. and Exposition, p.291-296.

Castro, M.S., Ayres H.M, da Costa, V.F., da Silva, L.C.P., 2007. Impacts of the SSSC control modes on small-signal and transient stability of a power system. *Electr. Power Syst. Res.*, **77**(1):1-9. [doi:10.1016/j.epsr.2006.01.003]

Chen, J., Lie, T.T., Vilathgamuwa, D.M., 2003. Enhancement of power system damping using VSC-based series connected FACTS controllers. *IEE Proc.-Gener. Transm. Distr.*, **150**(3):353-359. [doi:10.1049/ip-gtd:20030021]

da Cruz, J.J., Zanetta, L.C., 1997. Stabilizer design for multimachine power system using mathematical programming. *Int. J. Electr. Power Energy Syst.*, **19**(8):519-523. [doi:10.1016/S0142-0615(97)00023-9]

Dorf, R.C., Bishop, R.H., 2005. Modern Control Systems. Prentice Hall, New Jersey, USA, p.485-554.

Farsangi, M.M., Song, Y.H., Lee, K.Y., 2004. Choice of FACTS devices control inputs for damping inter-area oscillations. *IEEE Trans. Power Syst.*, **19**(2):1135-1142. [doi:10.1109/TPWRS.2003.820705]

Gyugyi, L., Schauder, C.D., Sen, K.K., 1997. Static synchronous series compensator: a solid-state approach to the series compensation of transmission lines. *IEEE Trans. Power Del.*, **12**(1):406-417. [doi:10.1109/61.568265]

Haque, M.H., 2005. Damping improvement by FACTS devices: A comparison between STATCOM and SSSSC. *Electr. Power Syst. Res.*, **76**(9-10):865-872. [doi:10.1016/j.epsr.2005.11.001]

Jowder, F.A.L., 2005. Influence of mode of operation of the SSSC on the small disturbance and transient stability of a radial power system. *IEEE Trans. Power Syst.*, **20**(2):935-942. [doi:10.1109/TPWRS.2005.846121]

Kazemi, A., Ladjevardi, M., Masoum, M.A.S., 2005. Optimal selection of SSSC based damping stabilizer parameters for improving power system dynamic stability using genetic algorithm. *Ir. J. Sci Technol. Trans. B Eng.*, **29**(B1):1-10.

Liu, S., 2006. Assessing Placement of Controller and Nonlinear Behavior of Electrical Power System Using Normal Form Information. PhD Thesis, Iowa State University, USA, p.128-133.

Noroozian, M., Ghandhari, M., Andersson, G., Gronquist, J., Hiskens, I.A., 2001. A robust control strategy for shunt and series reactive compensators to damp electromechanical oscillations. *IEEE Trans. Power Del.*, **16**(4):812-817. [doi:10.1109/61.956774]

Pourbeik, P., Gibbard, M.J., 1996. Damping and synchronizing torques induced on generators by FACTS stabilizers in multimachine power systems. *IEEE Trans. Power Syst.*, **11**(4):1920-1925. [doi:10.1109/59.544664]

Pourbeik, P., Gibbard, M.J., 1998. Simultaneous coordination of power system stabilizers and FACTS device stabilizers in a multimachine power system for enhancing dynamic performance. *IEEE Trans. Power Syst.*, **13**(2):473-479. [doi:10.1109/59.667371]

Sauer, P., Pai, M., 1998. Power System Dynamics and Stability. Prentice Hall, New Jersey, USA, p.123-159.

Vittal, V., 1992. Transient stability test systems for direct stability methods. *IEEE Trans. Power Syst.*, **7**(1):37-44. [doi:10.1109/59.141684]

Wang, H.F., 1999. Static synchronous series compensator to damp power system oscillation. *Electr. Power Syst. Res.*, **54**(8):113-119. [doi:10.1016/S0378-7796(99)00076-0]

Zanetta, L.C., da Cruz, J.J., 2005. An incremental approach to the coordinated tuning of power system stabilizers using mathematical programming. *IEEE Trans. Power Syst.*, **20**(2):895-902. [doi:10.1109/TPWRS.2005.846111]

Appendix A: Generator model (Sauer and Pai, 1998)

$$\dot{\delta} = \omega - \omega_s, \tag{A1}$$

$$M\dot{\omega} = P_m - P_e - D(\omega/\omega_s - 1), \tag{A2}$$

$$T'_{do}\dot{E}'_q = -E'_q - (X_d - X'_d)I_d + E_{FD}, \tag{A3}$$

$$T'_{qo}\dot{E}'_d = -E'_d + (X_q - X'_q)I_q, \tag{A4}$$

$$P_e = (I_d E'_d + I_q E'_q) + (X'_q - X'_d)I_d I_q. \tag{A5}$$

Appendix B: Used data for simulations

• Data of SSSC in the 4-machine system (in p.u. except indicated): T_{SSSC}=0.01 s, k=1, X_{SCT}=0.15, C_{DC}=1, V_{DCref}=1, X_{ref}=0.15, K_P=25, K_I=200.

• Data of SSSC in the 50-machine system (in p.u. except indicated): T_{SSSC}=0.01 s, k=1, X_{SCT}=0.15, C_{DC}=1, V_{DCref}=1, X_{ref}=0.15, K_P=15, K_I=170.

• Data of generators and network related to the 4-machine power system (Liu, 2006).

1. Synchronous generator data: Table B1.

2. Transmission line data: V_{base}=230 kV, S_{base}= 100 MV·A, X_{line}=0.001 p.u./km, R_{line}=0.0001 p.u./km.

3. Exciter parameters: Table B2.

4. Load flow data in p.u. (on system base 100 MV·A): Q_{C1}=2.551, Q_{C2}=2.54.3, Q_{L1}=2.50, Q_{L2}=2.5, P_{G1}=6.644, P_{G3}=6.644, P_{G4}=5, V_3=1.02∠0 (swing bus), $|V_1|$=1.02, $|V_2|$=1.02, $|V_4|$=1.02.

Table B1 Generator data (in p.u. except indicated)

Parameter	G_1	G_2	G_3	G_4
R_a	0.0025	0.0025	0.0025	0.0025
x_d	1.8	1.8	1.8	1.8
x_q	1.7	1.7	1.7	1.7
x'_d	0.3	0.3	0.3	0.3
x'_q	0.3	0.3	0.3	0.3
T'_{do} (s)	8	8	8	8
T'_{qo} (s)	0.4	0.4	0.4	0.4
H (s)	6.5	6.5	6.5	6.5
D	4	2	11	10
S_{base} (MV·A)	900	900	900	900

Table B2 Exciter data (in p.u. except indicated)

Generator	K_A	T_A	T_C	T_B	T_R
1	180	0.01	1	10	0.01
2	100	0.01	1	10	0.01
3	130	0.01	1	10	0.01
4	220	0.01	1	10	0.01